DOI: 10.1111/ede.12283

RESEARCH

WILEY EVOLUTION & DEVELOPMENT

Novel approach to quantitative spatial gene expression uncovers genetic stochasticity in the developing *Drosophila* eye

Sammi Ali[1] | **Sarah A. Signor**[1] | **Konstantin Kozlov**[2] | **Sergey V. Nuzhdin**[1,2]

[1] Molecular and Computational Biology, University of Southern California, Los Angeles, California

[2] Department of Applied Mathematics, St. Petersburg State Polytechnic University, St. Petersburg, Russia

Correspondence
Sarah A. Signor, Molecular and Computational Biology, University of Southern California, Los Angeles, CA.
Email: ssignor@usc.edu

Funding information
Foundation for the National Institutes of Health, Grant numbers: RO1GM102227, U01GM103804

Robustness in development allows for the accumulation of genetically based variation in expression. However, this variation is usually examined in response to large perturbations, and examination of this variation has been limited to being spatial, or quantitative, but because of technical restrictions not both. Here we bridge these gaps by investigating replicated quantitative spatial gene expression using rigorous statistical models, in different genotypes, sexes, and species (*Drosophila melanogaster* and *D. simulans*). Using this type of quantitative approach with molecular developmental data allows for comparison among conditions, such as different genetic backgrounds. We apply this approach to the morphogenetic furrow, a wave of differentiation that patterns the developing eye disc. Within the morphogenetic furrow, we focus on four genes, *hairy*, *atonal*, *hedgehog*, and *Delta*. Hybridization chain reaction quantitatively measures spatial gene expression, co-staining for all four genes simultaneously. We find considerable variation in the spatial expression pattern of these genes in the eye between species, genotypes, and sexes. We also find that there has been evolution of the regulatory relationship between these genes, and that their spatial interrelationships have evolved between species. This variation has no phenotypic effect, and could be buffered by network thresholds or compensation from other genes. Both of these mechanisms could potentially be contributing to long term developmental systems drift.

1 | INTRODUCTION

Variation in gene expression is the rule rather than the exception (Albert & Kruglyak, 2015; Bothma et al., 2014; Marinov et al., 2014; Pai et al., 2015; Signor & Nuzhdin, 2018). Variation in gene expression can come from perturbations in the environment, for example due to changes in temperature or maternal nutrition (Arsenault et al., 2018; Chen et al., 2015; Signor & Nuzhdin, 2018), and from differences in transcription between cells due to the burstiness of transcription (Bothma et al., 2014; Felix & Barkoulas, 2015). Organisms also experience perturbation in the form of recombination and new mutations. However, despite genetic and environmental perturbations to gene expression, organisms are able to produce robust phenotypic outcomes, suggesting that development is not readily affected by differences in gene expression (Garfield et al., 2013; MacNeil & Wallhout, 2011; Raj & van Oudenaarden, 2008; Romero et al., 2012). In contrast, on evolutionary timescales organisms must produce adaptive heritable variation in response to selection pressures, tapping those same sources of variation to which they might otherwise be robust. Indeed, the genetic basis of adaptation is often inferred to be due to differences in gene expression (Chan et al., 2010; Gompel, Prud'homme, Wittkopp, Kassner, & Carroll, 2005; Hoekstra & Coyne, 2007; Jeong et al., 2008;

Sammi Ali and Sarah A. Signor are co-first author.

Pai & Gilad, 2014; Signor, Liu, Rebeiz, & Kopp, 2016; Wray, 2007; Yassin et al., 2016). This balance between stability and lability is a question that has been addressed philosophically, but little experimental evidence exists to suggest the mechanisms underlying these phenomena (Casci, 2005; Gibson, 2009; Green et al., 2017; Heranz & Cohen, 2010; Hermisson & Wagner, 2004; Nijhout et al., 2017; Rutherford et al., 2007; Stern, 2000; True & Haag, 2001).

Genetic perturbations (differences in gene expression due to mutation or recombination) are the focus of this study, in contrast to other work such as that on cryptic variation that is interested in the interaction between mutations and the environment (Gibson & Reed, 2008; Paaby & Gibson, 2016; Paaby & Rockman, 2014). We use spatially resolved quantitative gene expression to gain a picture of variation in pathway components that cannot be understood from transcriptomics where many tissues have been combined, or single cell studies where gene expression variation due to genetic differences will be confounded with differences in transcription. From this we can understand how much genetically based gene expression variation we see in natural populations, where gene expression differences are either compensated by other genes in the pathway (Estes, Phillips, & Denver, 2011; Landry et al., 2005; Thompson, Zakon, & Kirkpatrick, 2015), mitigated by robust gene network structure (i.e., incoherent feed forward loops) (MacNeil & Walhout, 2011), or below threshold levels (Felix & Barkoulas, 2015). In addition, we focus on natural genetic variation within populations, which has long been the purview of evolutionary and population geneticists, while developmental biologists generally focus on the effect of large mutations in otherwise isogenic backgrounds (Paaby & Gibson, 2016, but see Lott et al., 2007).

The dearth of work on developmental variation in wildtype genetic backgrounds is in part because developmental approaches have long been restricted to data that is semi-quantitative (i.e., in situ hybridization, antibody staining). Indeed, gene expression studies are generally spatial or quantitative, but not both. In addition, the data is generally not interrogated from a quantitative perspective, including replication and rigorous statistical models. Without quantitative replication and statistical tests, one cannot effectively compare developmental processes among conditions, including health versus disease. This is especially important given the potential for complex interactions between conditionally neutral differences in gene expression to result in disease phenotypes. Here we use hybridization chain reaction (HCR) to bridge this gap between developmental and quantitative or population genetics by quantitatively measuring spatial gene expression in multiple genotypes from two sexes of two species (*Drosophila melanogaster* and *D. simulans*) (Choi, Beck, & Pierce, 2014). Furthermore, we introduce rigorous replication allowing for statistical hypothesis testing. Multiplexing of four genes simultaneously also allows straight forward analysis of gene co-expression, compared to other techniques that require inference across samples that have been individually stained. We use this substantial developmental dataset to focus on the well-known genes factors driving ommatidia specification the eye imaginal disc in *Drosophila* (Atkins et al., 2013; Li, Ohlmeyer, Lane, & Kalderon, 1995; Raj, van den Bogaard, Rifkin, van Oudenaarden, & Tyagi, 2008; Shah, Lubeck, Schwarzkopf, & He, 2016; Tsachaki and Sprecher, 2011).

The *Drosophila* eye is formed from an imaginal disc, which is initially patterned by a wave of differentiation marked by a visible indentation of the tissue, termed the morphogenetic furrow (MF). The MF passes from the posterior to the anterior of the disc over a period of two days (90 min per adjacent row of cells), giving each disc an element of both time and space in development (Figure 1) (Roignant & Treisman, 2009). A strength of the eye disc as a model is that within the MF all cells are arrested at G1, and there will be less additional variability introduced due to differences between cells in their stage of cell division (Baker & Yu, 2001; Escudero & Freeman, 2007; Firth & Baker, 2005; Firth, Bhattacharya, & Baker, 2010). Furthermore, by averaging across all cells within a row we reduce the impact of differences in transcriptional bursting across the eye disc (Bothma et al., 2014; Fukaya, Lim, & Levine, 2016; Tantale et al., 2016).

The furrow is initiated by *hedgehog,* which represses *hairy* within the MF and activates it indirectly in front of the MF through the long-range diffusion of *dpp* within the tissue (Figure 1) (Felsenfeld & Kennison, 1995; Fu & Baker, 2003; Strutt & Mlodzik, 1997). *hairy* represses *atonal*, preventing precocious neural development anterior to the MF (though this role has been recently contested) (Bhattacharya & Baker, 2012; Brown, Sattler, Markey, & Carroll, 1991; Brown, Sattler, Paddock, & Carroll, 1995). *hedgehog* activates the expression of *atonal*, driving the MF anteriorly (Figure 1) (Heberlein, Wolff, & Rubin, 1993; Ma, Zhou, Beachy, & Moses, 1993; Greenwood & Struhl, 1999). *atonal* is the proneural gene in *Drosophila*, establishing the competency to become photoreceptor cells (Jarman, Grell, Ackerman, Jan, & Jan, 1994). The relationship between *Delta/Notch* and the other members of the pathway is more complex, but it is clear that in cells posterior to the furrow *Delta/Notch* repress *atonal* (Figure 1) (Baker, Yu, & Han, 1996; Dokucu, Zipursky, & Cagan, 1996; Firth & Baker, 2005; Gavish et al., 2016). There is also some evidence that *Delta/Notch* repress negative regulators of *atonal* at the furrow, such as *hairy* (Baonza and Freeman, 2001; Bhattacharya & Baker, 2009; Brown et al., 1995). In addition, there is some evidence suggesting that *Delta/Notch* are involved in the early stages of *atonal* induction, and alternatively that *atonal* activates its own

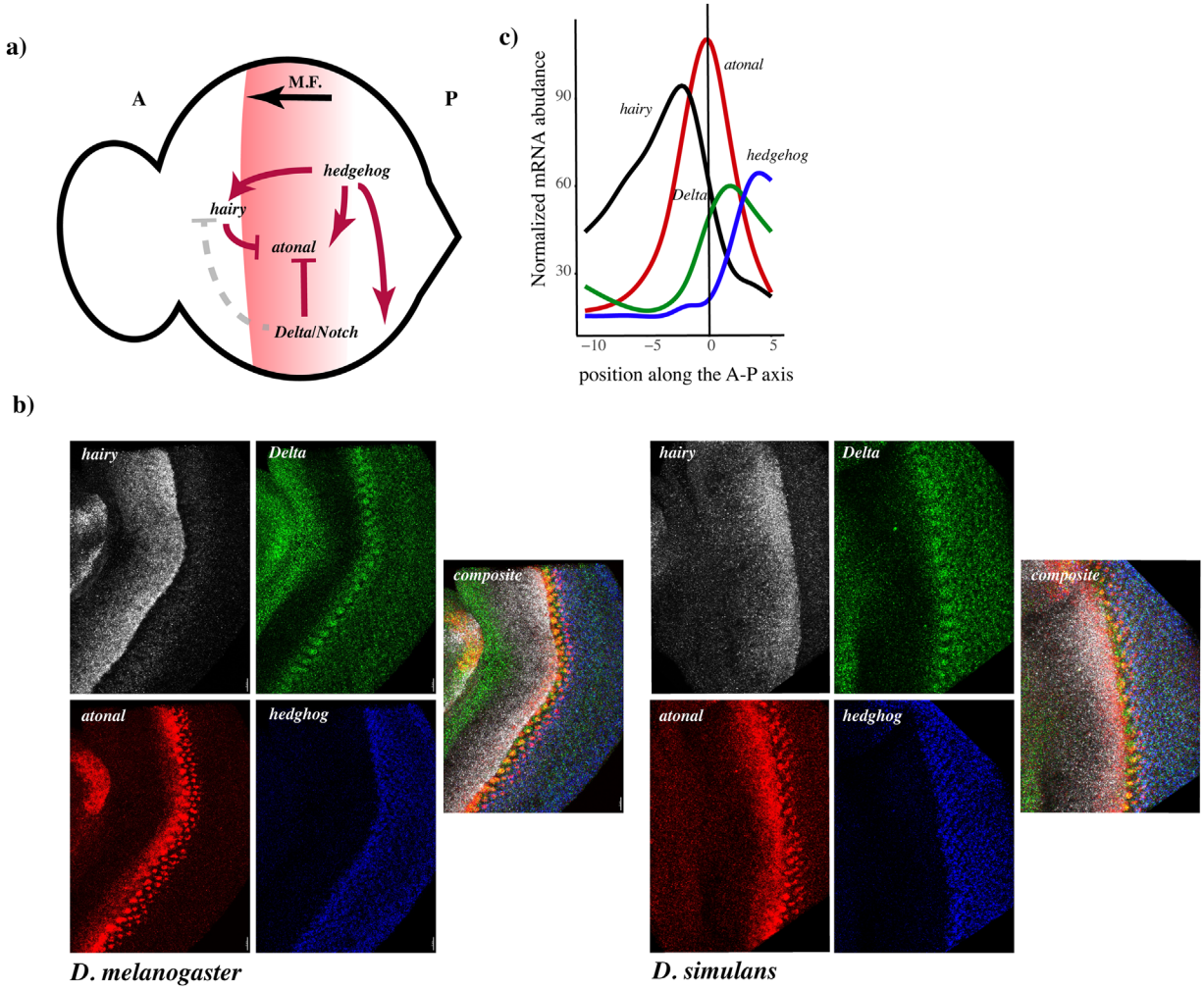

FIGURE 1 (a) A summary of the eye patterning genes and pathway explored in this paper. The position of the MF is shown in red, and its direction of movement indicated below. Regulatory relationships are illustrated either as repression (bar) or activation (arrow). Regulatory relationships which are unclear are shown as gray dotted lines. Note that *hairy* is activated by *hedgehog* at short range, and repressed by it indirectly at long range. Only the latter interaction is illustrated here. (b) Example images from the dataset, illustrating gene expression patterns of each gene. On the left is *D. melanogaster* and on the right *D. simulans*. Note that due to the different shapes of individual imaginal discs more of the antennal disc is shown for *D. melanogaster* than *D. simulans*, manifesting as a separate expression pattern to the left of each image. These areas were not included in the analysis, and indeed these expression patterns are shown prior to any image registration and are merely for illustrative purposes. The composite image makes the additional point that we were able to analyze co-expression patterns of all four genes without needing to stain each gene in different samples and infer gene co-expression patterns. (c) An illustration of the general expression pattern of each of the four genes in the study, along the anterior–posterior axis of the eye disc

transcription (Baker & Yu, 1997; Baker et al., 1996; Jarman et al., 1994; Li & Baker, 2001; Spencer, Powell, Miller, & Cagan, 1998; Sun, Jan, & Jan, 1998). *Delta/Notch* are expressed in the MF under the redundant control of *hedgehog* and *dpp* (Baonza & Freeman, 2001; Baonza & Freeman, 2005; Parks, Turner, & Muskavitch, 1995). There are many other genes involved in the specification of the eye disc that will not be mentioned here, in favor of focusing on the genes we have assayed. We analyze the spatial quantitative expression of *hedgehog*, *hairy*, *atonal*, and *Delta* to understand the evolving regulatory logic of the gene network and changes in spatial dynamics between sexes and species.

We term differences in gene expression between species, genotypes, and sexes "genetic stochasticity," as there are no phenotypic differences between these *Drosophila* eyes other than size and proportion of photoreceptor subtype (Hilbrant et al., 2014). We interpret genetic stochasticity in quantitative spatial patterns of gene expression in light of regulatory relationships among them. We approach a spatial and quantitative analysis of these gene expression patterns in three ways, first by explicitly creating a spatial gene expression profile and comparing between genotypes, sexes, and species. Second, we were interested in examining if the regulatory relationship between these genes had evolved between species

or harbors variation within a species. Lastly, we investigated the possibility that the spatial relationship between these genes relative to the MF had evolved or harbors variation within populations. These analyses summarize developmental data using quantitative genetic models, to uncover gene expression differences across tissues that would otherwise be undetected using conventional qualitative methods.

2 | METHODS

2.1 | Fly stocks

D. simulans were collected from the Zuma organic orchard in Zuma beach, CA in the spring of 2012 (Signor, New, & Nuzhdin, 2017). They were inbred by 15 generations of full sib crosses. *D. melanogaster* were collected in Raleigh, North Carolina and inbred for 20 generations (Mackay et al., 2012). Thus, any differences detected between species, sexes, or genotypes is due to natural variation.

2.2 | Staging and dissection of larvae

All flies were reared on a standard medium at 25°C with a 12-hr light/12-hr dark cycle. Five replicate eye discs were isolated from each of three strains, two sexes, and two species, for a total of 60 discs. Vials were used a single time for collection to avoid pseudo-replication, such that every genotype and sex was collected from a separate replicate population. Density of the cultures was controlled, as a standard number of parents were given two hours to lay their eggs. 120 hr after hatching, wandering 3rd instar larvae were placed in phosphate buffered saline (PBS) and separated by sex. Their guts were carefully removed posteriorly and their body was inverted anteriorly to expose the brains, eye discs and mouth hooks. After fixation and labeling (described below), eye discs were isolated and mounted. The MF moves one row every 90 minutes; thus, the expectation is that the MF will be consistently located within the same approximate location. Further, replicates were not conducted concurrently meaning that variation due to differences in timing will be randomly distributed across genotypes and sexes. If there are systematic differences in the position of the furrow, for example because there is some evidence that *D. simulans* develops approximately half a day more slowly than *D. melanogaster*, we test explicitly for an effect of the position of the morphogenetic furrow on gene expression in the following sections, for both species and sex (Génétique, 1983; Kuntz & Eisen, 2014).

2.3 | Hybridization chain reaction (HCR)

HCR is unique in that it produces gene expression patterns that are both quantitative and spatial. While other approaches such as FISH can be adapted to detect individual transcripts, HCR has a linear signal that is 20× brighter than FISH, it reduces non-specific background staining, and it can detect 88% of single RNA molecules in a cell with an appropriately low false discovery rate (Ma & Moses, 1995; Pan & Rubin, 1995). It is also highly repeatable, with different sets of probes targeted to the same gene showing correlations of .93–.99 (S. Fraser, pers. comm.). The DNA probes were designed and synthesized by Molecular Instruments (Choi et al., 2014) (S1 Table). Four genes were multiplexed in each preparation as orthogonally-designed hairpins allowed the simultaneous amplification of their target sequences (Figures 1 and S1). Each target mRNA was detected using five DNA probes to annotate the position and expression levels for each of the four assayed genes (*hairy, atonal, Delta and hedgehog*). Each probe contained two-initiator sequences (I1 and I2) that bound to a specific amplifier.

The protocol for HCR was modified from Choi et al. (2014) and is described briefly. The full protocol is available in S1 File. Inverted 3rd instar larvae were fixed in 4% paraformaldehyde diluted with PBS containing .2% Tween 20 (PBST). After fixation, larvae were washed with PBST, then increasing concentrations of methanol (30%, 70%, and 100%) at 25°C. Larva were stored in 100% methanol at −20°C. Methanol-fixed samples were thawed, washed with ethanol, re-permeabilized in 60% xylene, washed with ethanol, then methanol and rehydrated with PBST. Samples were permeabilized with proteinase K (4 mg/ml), fixed in 4% formaldehyde then washed with PBST at 25°C. Finally, at 45°C, samples were pre-hybridized for 2 hr before the addition of all the probes. The probe-hybridized larvae were placed in wash buffer (Molecular Instruments) at 45°C to remove excess probes. Fluorescently labeled hairpins were snap-cooled then added to the samples at 25°C and placed in the dark to amplify the signal. Afterwards, samples were washed in 5X SSCT solution, isolated in PBST, then placed in Prolong Gold antifade mounting medium (Molecular Probes).

2.4 | Microscopy

Three dimensional images of mounted, HCR stained 3rd instar larva eye discs were acquired on a Zeiss LSM 780 laser scanning microscope (Carl Zeiss MicroImaging, Inc., Thornwood, NY) with Objective Plan-Apochromat 63×/1.40 Oil. The gain was adjusted to avoid pixel saturation.

2.5 | Extraction of gene expression profiles

The first steps in the image analysis is bringing each image to the same orientation and segmenting it. Image segmentation produces a mask in which pixels are assigned to objects or background. Here the objects are one or several mRNA molecules. Then the cellular structure of the imaginal disc is

approximated using a hexagonal array. Though the real underlying cell structure of the imaginal disc is technically able to be recognized, this was unsatisfactory in our data due to imaging noise. Thus, at the second step using the R package hexbin we constructed a partition of the imaginal disc area into elements that represent pseudo-cells and have a biologically-relevant hexagonal shape (Brennan, Ashburner, & Moses, 1998). The number of pseudo-cells was selected by visual inspection of the combined image in which the hexagonal structure was overlaid onto the *atonal* channel to verify fit. We are primarily interested in expression profiles around the MF, providing us a convenient landmark to align images from different preparations, thereby assigning coordinates to the pseudo-cells. However, deformations of the eye disc during growth and preparation sometimes distorts the MF. We used splines to correct for any bending or deformation of the MF. We note that the use of pseudo-cells could potentially result in gene expression from single cells being segregated into multiple cells and vice versa, however as it effects all genes equally in a given locale, this should have little effect on the outcome of the analysis. Next, using the histograms of cumulative pixel intensities of objects in expression domains and non-expressing areas we estimated the typical intensity of a transcript and typical background signal, respectively. Consequently, the cumulative intensities greater than the background are divided by the intensity attributed to single mRNA molecule to yield counts of mRNA molecules. This normalizes the expression profiles and corrects for differences in microscope gain between images. Finally, the gene expression profiles are estimated for every pseudo-cell.

2.6 | Morphological reconstruction and contrast mapping segmentation

To detect gene transcripts within the image stacks we applied a version of the MrComas method that was modified for processing 3D images (Please see S2 Figure for an illustration of the different steps in the process described below, in addition Kozlov et al., 2017 provides a more thorough description of the process). This approach first enhances contrast within the image and reduces noise. The images were enlarged by a factor of four with the nearest-neighbor algorithm. They were processed by morphological reconstruction using both opening and closing, where closing (opening) is dilation (erosion) that removes extraneous dark (bright) spots and connects bright (dark) objects (Vincent, 1993). The contrast mapping operator assigns each pixel the maximum value between the pixel-by-pixel difference of the reconstructed images and their pixel-by-pixel product and produces the rough mask for each channel. An image, I, is mapping from a finite rectangular subset L onto the discrete plane Z^2 into a discrete set 0, 1, . . ., N − 1 of gray levels. y denotes the pixel of an image I inside a structural element B. Let the dilation $\delta_B$and erosion ϵ_B by structural element B be defined as:

$$\delta_B(I) = {}_{\gamma\epsilon_B}I(y) = I\ B\ \epsilon_B(I) = {}_{\gamma\epsilon_B}I(y) = I\ B \qquad (1)$$

where ∨ and ∧ denote infimum and supremum respectively. Then formulae:

$$\delta^1_{I,B}(J) = (J\ B)\ I\ \varepsilon^1_{I,B} = (J\ B)\ I \qquad (2)$$

denote geodesic dilation $\delta^1_{I,B}$ and erosion $\varepsilon^1_{I,B}$. Binary reconstruction extracts those connected components of the mask image which are marked on the marker image, and in grayscale it extracts the peaks of the masked image marked by the marker image. Using the dilated masks image I as the marker $J : J = \delta_B(I)$ defines closing by reconstruction:

$$\gamma_B(I) = \varepsilon^1_{I,B}\varepsilon^1_{I,B}\ldots\varepsilon^1_{I,B}[\delta_B(I)] \qquad (3)$$

Opening by reconstructions uses eroded mask I as a marker J:

$$\phi_B(I) = \delta^1_{I,B}\delta^1_{I,B}\ldots\delta^1_{I,B}[\varepsilon_B(I)] \qquad (4)$$

Then the difference between closing and opening by reconstruction has the meaning of the gradient:

$$\nabla_B(I) = \gamma_B(I) - \phi_B(I) \qquad (5)$$

To create strong discontinuities at object edges and flatten signal with the objects the contrast mapping operator takes a maximum between the difference and the pixel-by-pixel produce of the reconstructed images and produces a rough mask for each channel:

$$R = \max\{\nabla_B(I),\gamma_B(I)\ \phi_B(I)\} \qquad (6)$$

Subsequently, this mask was subjected to distance transform, which substituted each pixel value with the number of pixels between it and the closest background pixel. This operation creates “peaks” and “valleys” of intensity inside foreground objects. To split erroneously merged objects watershed transform was applied, which treats the whole image as a surface and intensity of each pixel as its height and determines the watershed lines along the tops of ridges separating the catchment basins (Meyer, 1994). The quality of segmentation is assessed visually by inspection of the object boarders overlaid with the original image. Finally, each mask is returned to its original size and quantitative measures are made of shape and intensity characteristics such as the number of pixels, as well as their mean and standard deviation in the detected object. MrComas is free and open

source software available at http://sourceforge.net/p/prostack/wiki/mrcomas. Application of MrComas to synthetic images to evaluate performance and comparison to existing methods are described in Kozlov et al. (2017).

2.7 | Approximating the MF

We defined the position of the MF as the location of maximum *atonal* expression. The shape of the MF was approximated with a spline using function smooth.spline in R. The degrees of freedom and other parameters were chosen to make the approximation coincide visually with a MF image.

2.8 | Inferring counts of transcript number

Segmentation of the image provided a table of coordinates and the shape and intensity characteristics of detected transcripts. Here, we applied filtering steps to remove false positives and determine the count of mRNA transcripts. First, we assumed the object we detected as least intense but most frequent corresponds to a single mRNA molecule. Then, we inferred background intensity for objects outside of well-annotated domains of expression of the four genes. Assuming that the majority of true objects contain a single molecule, we compare the distribution of cumulative intensities of particles in expression domains and areas of known non-expression to obtain the typical intensity of a true single molecule and a false positive, respectively. All detected signals that were lower than the typical intensity of a false positive were removed from the dataset. The number of removed objects is typically less then 10%. All other cumulative pixel intensities were divided by the typical intensity of a true single molecule as normalization coefficient to yield an estimate of the number of mRNA transcripts.

2.9 | Image registration

We applied an affine coordinate transformation to each eye disc to make the corresponding maxima and the width of expression patterns of four genes in different eyes coincide as closely as possible. To do so, we shifted the coordinate system of each eye to its center and also scaled them in the A-P direction. The center of the pattern in A-P direction is the MF. This aligns the position of maximum *atonal* expression (defined as the center of the MF), such that gene expression patterns can be compared across discs.

We mapped the expression patterns to a unified hexagonal structure in order to make comparisons between pseudo-cells from individual imaginal discs. The unified cell structure was constructed using the R package hexbin. Each cell in the unified grid represents an "average" cell from individual eyes. The size of a hexagon in the unified grid is greater or equal than the cell size in the individual eye. Thus, the number of molecules in each unified cell in the mapped pattern equals the mean over the cells from native pattern that are covered by this unified cell. After such coordinate transformation, the MF region is defined as 20 cells on either side of the MF, to focus the analysis on the area of interest (the MF).

2.10 | Filtering and quality controls for each eye disc

Some eye imaginal discs were damaged or deformed in the process of dissection or mounting, resulting in regions of erroneous gene expression, such as disruptions to the MF. The expression profile of each disc was examined by eye and these regions were individually trimmed out of the final dataset. At the edges of each eye disc the pattern of the MF was also degraded, so each eye disc was trimmed dorso-ventrally prior to analysis. Five outliers were excluded from the dataset of 60 discs, determined as a single member of the five replicates per genotype/sex with more than a 3× difference in expression values. This resulted in a final dataset of 55 eye discs.

There are no phenotypic differences between the eyes of *D. melanogaster* and *D. simulans* other than size and proportion of photoreceptor subtype. Size is included as a co-factor in the relevant models discussed below, and results only in a larger area being patterned for ommatidia rather than a difference in pattern. In addition, photoreceptor subtype is not determined or affected by the genes expressed during the initial patterning phase in the MF (Cook, Pichaud, Sonneville, Papatsenko, & Desplan, 2003; Johnston and Desplan, 2014; Johnston et al., 2011; Wernet et al., 2006).

2.11 | Analysis of individual spatial gene expression patterns

We were primarily interested in variation in gene expression profiles across the eye disc, that is using differences in expression averaged across rows along the *x*-axis. While the *y*-axis is of interest, variation in the shape, size, degree of deformation, and occasional damage to the disc made this analysis intractable. We fit curves to each gene expression profile using the mgcv package in R, using a generalized additive model with integrated smoothness estimation. Smoothing terms are represented using penalized regression splines. predict.gam was used to fit the curves to the original range of values and down sample the curves to eight points. MANOVAs were performed using the "Pillai" test for species × genotype × sex.

2.12 | Modeling framework to understand variation and evolution of the eye patterning gene network

We wanted to understand if variation existed within the regulatory logic of *hairy*, *atonal*, *Delta*, and *hedgehog*, or if

there had been evolution between species. To understand the regulatory logic between genes we focused on biologically relevant relationships, such as the regulation of *hairy* by *Delta* and *hedgehog*, but excluded such relationships as *hairy* and *atonal*. This was due to the low overlap between *hairy* and *atonal* expression domains, where including cells where only one or another was expressed would artificially create a relationship between expression levels. Both *hairy* and *atonal* are downstream, directly or indirectly, of *Delta* and *hedgehog* thus it was these relationships that were modeled. We limited the analysis to cells where all genes included were expressed in at least ten molecules.

In the previous analysis, we investigated variation in the cryptic spatial quantitative expression pattern of genes in the MF. Here, we will investigate the possibility that genes in the MF have evolved, or harbor variation, for how they affect each other in particular cells. For example, is high *atonal* expression associated with high expression of *hedgehog*, given that *hedgehog* activates *atonal*? We used the following equations to determine the relationship between the expression of these genes:

$$hairy(i,s) = k^{Dl} \times Dl(i,s) + k^{hh} \times hh(i,s) + \alpha \quad (7)$$

$$atonal(i,s) = k^{Dl} \times Dl(i,s) + k^{hh} \times hh(i,s) + \alpha \quad (8)$$

The coefficient k and constant α were fit using standard methods for multiple regression. Here *hairy*(*i*,*s*) and *atonal*(*i*, *s*) are the measured expression level of each gene in cell *i* in individual *s*. Dl(*i*,*s*) and hh(*i*,*s*) are vectors containing the corresponding expression levels of *hairy* and *atonal*'s regulators *Delta* and *hedgehog*. To determine if the regulatory logic is the same between genotypes and species we can then use the regression coefficients from these models in a MANOVA. We note that we cannot exclude the possibility that other unmeasured genes are responsible for producing this variation.

2.13 | Model for understanding overall variation and evolution of MF structure

Lastly, we wanted to understand if there is variation in the relationship between the MF and gene expression, or if variation existed for the size of the MF overall. Two processes occurred to make the MF comparable between samples, the MF was shifted to occupy the same position depending upon the position of maximum *atonal* expression, and the MF was scaled to occupy the same total area. If the MF was consistently in a different position for different species, sexes, or genotypes, meaning that the amount it needed to be shifted such that the center of the MF occupied the same location was consistently different for different factors, this might imply genetically based differences in the rate at which the MF proceeds. We performed an ANOVA in R using the amount that each disc was shifted to test for systemic differences in MF position. To test for differences in the amount that each disc was scaled, we need to control for differences in size in the original disc, as the scaling factor will depend both on the size of the original disc and the width of the MF relative to the disc. To account for differences in size we include the number of rows of cells in the original eye disc as a cofactor and perform ANOVA in R (Figure S2). The number of rows of cells is estimated along the D-V axis in the entire eye disc by the R program hexbin, and is not restricted to the region surrounding the MF.

3 | RESULTS

3.1 | Individual spatial gene expression patterns

First, to characterize the spatiotemporal dynamics of transcriptional activity along the anterior-posterior axis, we took the spatial average of signal across the dorsal-ventral axis and compared between genotypes, sexes, and species (Figure 2a, we note that the smoothed curves in the figures were created using smooth.spline in ggplot2, which is not the same method for curve fitting as in the analysis). We found abundant spatial quantitative variation in expression profiles (Figures 2–3). The expression profile of *hairy* around the MF harbors variation between genotypes and there is an interaction between genotype and sex (Table 1, $p = 2 \times 10^{-3}$, $p = 0.02$). There has also been evolution between species for *hairy* (Table 1, $p = 3 \times 10^{-4}$). While *atonal* has not evolved between species, there is variation in expression profile between genotypes, sexes, and there is an interaction between genotype and sex (Figures 3a–3c, Table 1, Figure S2, $p = 4 \times 10^{-4}$, $p = .02$, $p = .02$). Surprisingly, given the conservation of *Delta* in general, *Delta* harbors variation in spatial quantitative expression behind the MF between genotypes and sexes (Table 1, $p = 2 \times 10^{-3}$, $p = 7 \times 10^{-4}$) and there are significant interactions between genotype and sex (Figures 2b and 2c, Table 1, $p = 2 \times 10^{-3}$). There has also been evolution of *Delta* between species, and evolution of the interaction between species and sex (Table 1, Figure S2, $p = .03$, $p = 3 \times 10^{-4}$). *hedgehog* is not different between species but is significantly different between genotypes, sexes, and there is an interaction between the two (Table 1, $p = 5 \times 10^{-4}$, $p = .05$, $p = 1 \times 10^{-3}$). There is also a significant interaction between species and sex (Table 1, $p = .01$).

Thus, *hairy* and *Delta* have evolved different spatial quantitative expression patterns between species, while *Delta*, *atonal*, and *hedgehog* harbor variation between genotypes and sexes. Given that there are regulatory

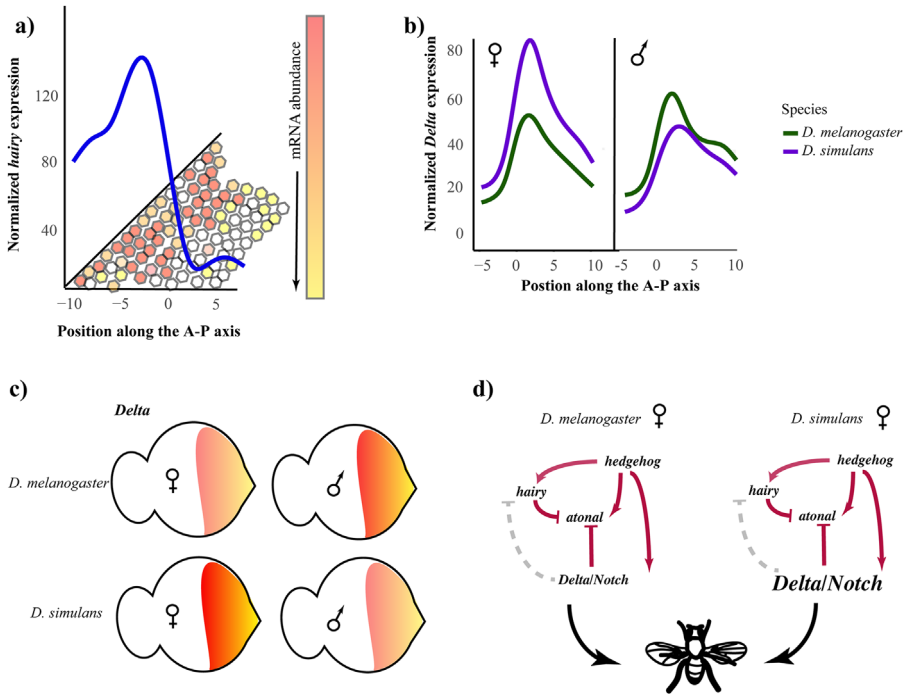

FIGURE 2 (a) This is an example of a curve being fitted to the gene expression profiles, though note that the curve corresponds to the average in a given row (*x*-axis). The hexagons are intended to represent cells with varying amounts of *hairy* expression, from the highest (red) to the lowest (white). (b) An illustration of variation in *Delta* expression between species and sexes. Curves shown are fitted to all genotypes within a sex and species. (c) An illustration using the imaginal disc of how *Delta* expression varied between species and sexes, with lower expression in *D. melanogaster* females and *D. simulans* males (d) Evolution of *Delta* illustrated within the context of the gene network, illustrating how changes in *Delta* expression are not perturbing the gene network and result in phenotypically normal *Drosophila*

relationships between these genes, it is interesting to see that they do not all harbor variation for the same factors. This could potentially be due to the influence of other unmeasured regulatory factors, or to variation in the relationship between these genes and other components in the gene regulatory network. However, whatever the source of "buffering" of the network, be it the effect of other genes or threshold effects on development, the fact that this information is not retained within the steps of the pathway supports our supposition that this variation does not ultimately have a phenotypic effect (see section 4).

3.2 | Variation and evolution of the eye patterning gene network

The regulatory effects between genes can be discerned from the degree of quantitative co-localization, and variation in this co-localization between species, genotypes, and sexes. There has been evolution in the regulatory logic of *hairy* and its upstream regulators *Delta* and *hedgehog* between species (Figure 4, Table 2, $p = .03$, see S2 File for the r^2 values from the individual regressions). There is also variation between sexes in the regulatory logic of *hairy* and its upstream regulators *Delta* and *hedgehog* (Table 2, $p = .03$). There has been significant evolution of the regulatory logic of *atonal*, in a significant interaction between species and sex (Figure S3, $p = 1 \times 10^{-3}$). Furthermore, while there was no significant effect of genotype for *hairy*, there is for *atonal*, indicating that there is variation segregating in the population affecting the relationship between *atonal, hedgehog*, and *Delta* ($p = 1.6 \times 10^{-5}$, see S3 File for the r^2 values from the individual regressions). There is also a significant interaction between genotype and sex ($p = 1 \times 10^{-3}$). Thus, the relationship between *hairy* and *atonal* and their regulators has evolved between species and sexes in *hairy*, and between genotypes and sex in *atonal*. We illustrate this difference between species in Figure 4, where a different relationship between *hairy* and *hedgehog* is visible between *D. melanogaster* and *D. simulans*. In brief, the frequency of cells with a given log transformed level of expression are plotted against one another for *hairy* and *hedgehog*. *hairy* is primarily expressed anterior to the MF and *hedgehog* posterior, and they have a different regulatory relationship in each region with *hedgehog* activating *hairy* indirectly at long range (anterior) and repressing it short range (posterior). This is reflected in the frequency of cells expressing both genes for *D. melanogaster*, where anterior to the MF there is a high frequency of *hairy* expressing cells and a low frequency of co-occurring high *hedgehog* expression. Posterior to the MF the opposite is true, with high expression of *hedgehog*

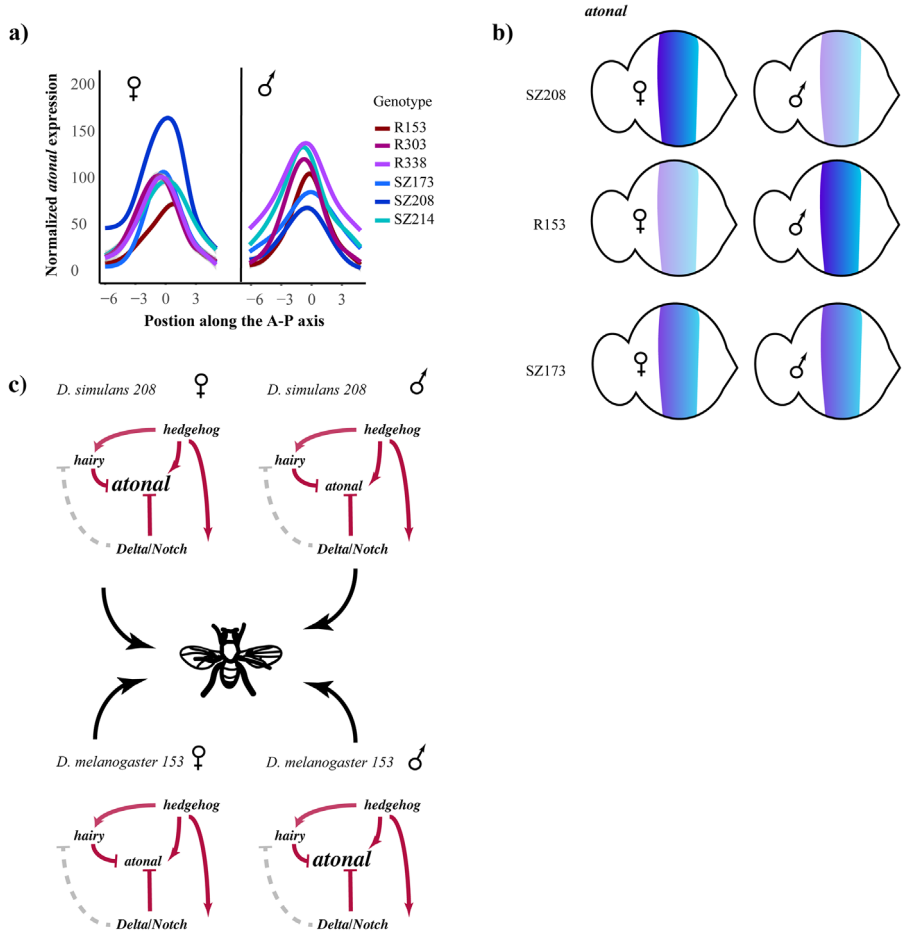

FIGURE 3 (a) An illustration of variation in *atonal* expression between genotypes and sexes. Curves shown are fitted to each genotype and sex. (b) An illustration using the imaginal disc of how *atonal* expression varied between genotypes, with lower expression in females of *D. melanogaster* R153 and males of *D. simulans* Sz208. *D. simulans* Sz173 has lower expression than females of Sz208 but it is not sexually dimorphic. (c) Evolution of *atonal* illustrated within the context of the gene network, illustrating how changes in *atonal* expression are not perturbing the gene network and result in phenotypically normal *Drosophila*

lacking concordance with any expression of *hairy*. In *D. simulans*, posterior to the MF, this relationship is the same as in *D. melanogaster*. However, in anterior to the MF this is not the case. Expression of *hairy* and *hedgehog* both increase as the other increases, with widespread co-occurrence.

3.3 | Variation and evolution of MF structure

The amount that the eye discs were shifted is not significant for genotype, sex, or species. This suggests that any differences in development time are not significant between

TABLE 1 The results of the MANOVA for species × genotype × sex for each gene

hairy

Effect	numDF	denDF	F-value	p-value
Species	8	35	5.1	**3×10^{-4}**
Genotype	32	152	2.07	**2×10^{-3}**
Sex	8	35	1.08	0.32
Species x Sex	8	35	1.94	0.08
Genotype x Sex	32	152	1.73	**0.02**

atonal

Effect	numDF	denDF	F-value	p-value
Species	8	35	1.53	0.18
Genotype	32	152	2.31	4×10^{-4}
Sex	8	35	2.6	0.02
Species x Sex	8	35	1.91	0.09
Genotype x Sex	32	152	1.73	**0.02**

Delta

Effect	numDF	denDF	F-value	p-value
Species	8	35	2.43	**0.03**
Genotype	32	152	2.07	**2×10^{-3}**
Sex	8	35	4.55	**7×10^{-4}**
Species x Sex	8	35	5.03	**3×10^{-4}**
Genotype x Sex	32	152	2.03	**2×10^{-3}**

hedgehog

Effect	numDF	denDF	F-value	p-value
Species	8	35	0.87	0.55
Genotype	32	152	2.28	5×10^{-4}
Sex	8	35	2.23	0.05
Species x Sex	8	35	2.88	0.01
Genotype x Sex	32	152	2.17	1×10^{-3}

Significant *p*-values are indicated in bold with gray shading.

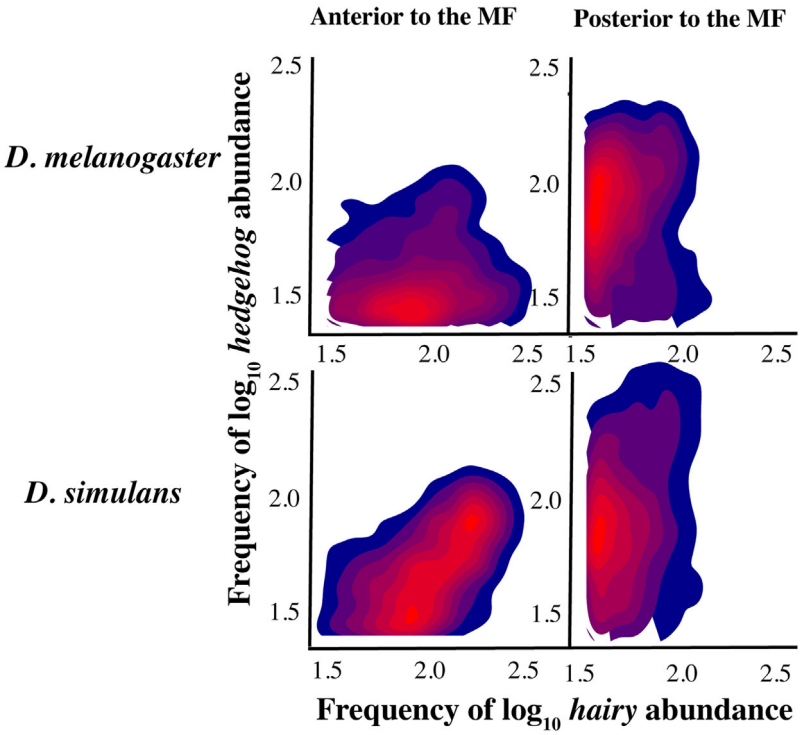

FIGURE 4 An example of variation in regulatory logic between *D. simulans* and *D. melanogaster* for *hairy* and *hedgehog*. The heat map illustrates the density of points, and thus reflects the frequency of a given co-expression profile between *hairy* and *hedgehog*. Gene expression values were log-transformed to better illustrate lower values and split between anterior to the MF and posterior to the MF. The split between the two regions was to investigate the possibility that *hedgehog* had a different regulatory relationship with *hairy* depending upon its relationship to the MF, given that *hedgehog* is thought to activate *hairy* long range (indirectly) and repress *hairy* short range

species, genotype, or sex, and/or that the exact position of the furrow is not having an effect on these gene expression patterns. However, the amount that they were scaled is, after accounting for original differences in size, between species ($p = 1.38 \times 10^{-6}$). This suggests that the total relative width of the MF varies between species, but not between genotypes or sexes. This is also suggestive of evolving interrelationships among genes that could result in broader

TABLE 2 The results of the MANOVA for species × genotype × sex for the regulatory relationship between *hairy*, *Delta*, and *hedgehog*, and *atanol*, *Delta*, and *hedgehog*

hairy

Effect	*numDF*	*denDF*	F-value	*p*-value
Species	2	41	4.03	**0.025**
Genotype	8	84	1.2	0.31
Sex	2	41	3.95	**0.027**
Species x Sex	2	41	0.78	0.46
Genotype x Sex	8	84	1,11	0.37

atonal

Effect	*numDF*	*denDF*	F-value	*p*-value
Species	2	41	2.64	0.08
Genotype	8	84	5.43	**1.6×10^{-5}**
Sex	2	41	0.67	0.52
Species x Sex	2	41	8.09	**1×10^{-3}**
Genotype x Sex	8	84	2.41	**0.02**

Significant *p*-values are indicated in bold with gray shading.

or narrower areas in which they enhance or suppress expression of one another.

4 | DISCUSSION

We present here a replicated, quantitative, and spatially explicit analysis of the expression of genes driving cell differentiation in the *Drosophila* eye. Our results summarize a complicated pattern of variation sorting in the gene network involved in patterning the MF. For example, the overall shape of the expression of *hedgehog* across the eye disc is different between genotypes, sexes, and there is an interaction between species and sex and genotype and sex. *hedgehog* upregulates *hairy*, but *hairy* has differences in expression between species (which *hedgehog* does not), genotypes, and there is an interaction between genotype and sex. Thus, the differences seen in upstream regulators, such as *hedgehog*, are not recapitulated in their downstream targets. In another example, *Delta/Notch* is expected to repress *atonal*, but while *Delta/Notch* is significant for all categories tested *atonal* is only significant for genotype, sex, and their interaction. It is possible that this variation is being mitigated or dampened by other regulatory factors not assayed here, or that certain aspects of genetic background are more or less sensitive to variation. For example, fixed variation between species could dampen variation at *Delta/Notch* while sorting variation remains sensitive between genotypes, which propagates to *atonal*.

It may be that all of this variation is within levels tolerated by the network, as it has been shown that gene networks can have thresholds of variation, below which differences in expression are effectively neutral. These thresholds can also be two sided, creating a sigmoidal curve the center of which is neutral phenotypic space (Felix & Barkoulas, 2015). Many studies have shown a relative insensitivity to variation in gene dosage, for example, in *Drosophila* early embryos the *bicoid* gradient results in normal development at one to four dosages of the gene, but markedly abnormal development at six or more (Liu, Morrison, & Gregor, 2013; Lucas et al., 2013; Namba, Pazdera, Cerrone, & Minden, 1997). It is also possible that the "genetic stochasticity" documented in these genes is in fact deleterious, and is being compensated for elsewhere in the network. While most deleterious mutations are purged by selection, they may rise in frequency due to genetic drift or hitchhiking, among other possible causes (Burch & Chao, 1999; Chun & Fay, 2011; Estes & Lynch, 2003; McKenzie & Clarke, 1988). This type of compensatory mutation has been documented in microbial and animal systems (Burch & Chao, 1999; Brown et al., 2010; Charusanti et al., 2010; Estes & Lynch, 2003; Estes et al., 2011; Maisnier-Patin & Andersson, 2004; McKenzie, 1993; McKenzie, Whitten, & Adena, 1982; Moore, Rozen, & Lenski, 2000; Stoebel, Hokamp, Last, & Dorman, 2009; Szamecz et al., 2014). Recently cell cycle heterogeneity has been implicated in the appearance of widespread noise in development, however this is likely not responsible for the genetic stochasticity observed here as the majority of MF cells assayed here are arrested at G1 (Keren et al., 2015; Kumar, 2013).

The differences in the co-expression patterns of *hairy*, *atonal*, and their upstream regulators *hedgehog* and *Delta/Notch* may represent the early stages of developmental systems drift, where pathway components can evolve different relationships while maintaining the same phenotypic output (True & Haag, 2001). This type of "quantitative developmental systems drift" has been proposed to be a pervasive feature of evolving developmental systems (Crombach et al., 2016; Wotton et al., 2015). It may also be that the overall relationship between the genes has not evolved, but that variation between the network components is beneath some critical threshold that would results in differences in downstream regulation—that is that co-expression patterns may show evolution and variation, but the basic inputs and outputs of the network are conserved. These are not fundamentally different ideas, rather they may represent different points on an evolutionary continuum. If developmental systems drift is at work, it could potentially be due to changes in these critical thresholds, for example if the threshold is lower in one species then less of an upstream gene is needed to create the same output. The evolution and maintenance of expression thresholds and developmental systems drift is potentially an interesting area of future research.

There have been other semi-quantitative approaches to studying spatial gene expression patterns. In another study on *orthodenticle*, the authors found that the spatial and temporal pattern of gene expression was conserved but the amount of gene product was not, though this work was not strictly quantitative given that measurements were from in situ hybridization and reporter constructs and there was no rigorous statistical testing (Goering et al., 2009). This is in contrast to our results which showed significant differences in the spatial relationship between gene expression patterns between species. Other semi-quantitative works on the *Drosophila* embryo using in situ hybridization found that the regulatory relationship between genes in the anterior-posterior blastoderm patterning network were conserved, despite differences between species in their spatio-temporal pattern (Fowlkes et al., 2011; Wunderlich et al., 2012). Here we find that the regulatory relationship between *atonal* and *hairy*, and their regulators *hedgehog* and *Delta*, has evolved between species, sexes, and genotypes.

One of the important messages from this work is that rigorous statistical testing can uncover molecular variation in spatial and quantitative developmental gene expression. Using the type of replication applied in quantitative genetics with developmental data we were able to apply rigorous statistical models to micro-evolutionary variation in

development. Despite this variation, observed with repeatable observations of developmental patterns among natural genotypes, the phenotypes of all flies are normal. This points to a potential abundance of hidden noise in spatial and quantitative gene expression. The evolutionary approach to development generally targets large changes that have occurred over broad phylogenetic distances (Ito et al., 2013; Jeong et al., 2008; Kopp, Duncan, Godt, & Carroll, 2000; Reed et al., 2011; Rosenblum, Römpler, Schöneberg, & Hoekstra, 2010; Signor et al., 2016; Yassin et al., 2016). Accordingly, the presence of abundant underlying variation is perhaps not a huge surprise. But it does have large implications, as it suggests that developmental models should be modified so that such abundant genetic variation is buffered from perturbing the final phenotype. In the future, application of this type of replicated, quantitative, spatially resolved data will have unique insights into the penetrance of disease phenotypes and the origin of developmental defects.

DATA AVAILABILITY

All data associated with the manuscript can be found at: https://doi.org/10.5061/dryad.410t5.

AUTHORS' CONTRIBUTIONS

SA performed the staining and imaging of the eye discs, KK processed the imaging data, SS conceived of the experiment, analyzed the processed data and wrote the paper, SN conceived of the experiment and coordinated the research.

ACKNOWLEDGMENTS

The authors thank S. Restrepo, M. Samsonova, A. Kopp, P. Marjoram, J. Butler, G. Mackerel, R. Hudson, E. Williams, A. Lana, S. G. Frusina, H. Cagni, and R. Hess for help with experimental procedures and manuscript preparation. This work was supported by grants U01GM103804 and RO1GM102227 to S.N.

CONFLICT OF INTEREST

The authors declare no conflicts of interest.

ORCID

Sarah A. Signor http://orcid.org/0000-0003-2401-0644

REFERENCES

Albert, F., & Kruglyak, L. (2015). The role of regulatory variation in complex traits and disease. *Nature Reviews Genetics*, *16*, 197–212.

Arsenault, S. V., Hunt, B. G., & Rehan, S. M. (2018). The effect of maternal care on gene expression and DNA methylation in a subsocial bee. *Nature Communications*, *9*, 3468.

Atkins, M., Jiang, Y., Sansores-Garcia, L., Jusiak, B., Halder, G., & Mardon, G. (2013). Dynamic rewiring of the *Drosophila* retinal determination network switches its function from selector to differentiation. *PLoS Genetics*, *9*, e1003731.

Baker, N. E., Yu, S., & Han, D. (1996). Evolution of proneural *atonal* expression during distinct regulatory phases in the developing Drosophila eye. *Current Biology*, *6*, 1290–1301.

Baker, N. E., & Yu, S. Y. (2001). The EGF receptor defines domains of cell cycle progression and survival to regulate cell number in the developing *Drosophila* eye. *Cell*, *104*, 699–708.

Baker, N. E., & Yu, S. Y. (1997). Proneural function of neurogenic genes in the developing *Drosophila* eye. *Current Biology*, *7*, 122–132.

Baonza, A., & Freeman, M. (2001). Notch signalling and the initiation of neural development in the *Drosophila* eye. *Development*, *128*, 3889–3898.

Baonza, A., & Freeman, M. (2005). Control of cell proliferation in the *Drosophila* eye by *Notch* signaling. *Developmental Cell*, *8*, 529–539.

Bhattacharya, A., & Baker, N. E. (2012). The role of the bHLH protein *hairy* in morphogenetic furrow progression in the developing *Drosophila* eye. *PLoS ONE*, *7*, e47503.

Bhattacharya, A., & Baker, N. E. (2009). The HLH protein *Extramacrochaetae* is required for R7 cell and cone cell fates in the *Drosophila* eye. *Developmental Biology*, *327*:288–300.

Bothma, J. P., Garcia, H. G., Esposito, E., Schlissel, G., Gregor, T., & Levine, M. (2014). Dynamic regulation of eve stripe 2 expression reveals transcriptional bursts in living *Drosophila* embryos. *Proceedings of the National Academy of Sciences of the United States of America*, *111*, 10598–10603.

Brennan, C. A., Ashburner, M., & Moses, K. (1998). Ecdysone pathway is required for furrow progression in the developing *Drosophila* eye. *Development*, *125*, 2653–2664.

Brown, K. M., Costanzo, M. S., Xu, W., Roy, S., Lozovsky, E. R., & Hartl, D. L. (2010). Compensatory mutations restore fitness during the evolution of Dihydrofolate reductase. *Molecular Biology and Evolution*, *27*, 2682–2690.

Brown, N. L., Sattler, C. A., Markey, D. R., & Carroll, S. B. (1991). *Hairy* gene function in the *Drosophila* eye: Normal expression is dispensable but ectopic expression alters cell fates. *Development*, *113*, 1245–1256.

Brown, N. L., Sattler, C. A., Paddock, S. W., & Carroll, S. B. (1995). *Hairy* and *emc* negatively regulate morphogenetic furrow progression in the *Drosophila* eye. *Cell*, *80*, 879–887.

Burch, C. L., & Chao, L. (1999). Evolution by small steps and rugged landscapes in the RNA virus phi6. *Genetics*, *151*, 921–927.

Casci, T. (2005). Robust arguments about canalization. *Nature Reviews*, *6*, 89.

Chan, Y. F., Marks, M. E., Jones, F. C., Villarreal, G., Shapiro, M. D., Brady, S. D., … Kingsley, D. M. (2010). Adaptive evolution of pelvic reduction in sticklebacks by recurrent deletion of a *Pitx1* enhancer. *Science*, *327*, 302–305.

Charusanti, P., Conrad, T. M., Knight, E. M., Venkataraman, K., Fong, N. L., Xie, B., … Palsson, B. (2010). Genetic basis of growth adaptation of *Escherichia coli* after deletion of *pgi*, a major metabolic gene. *PLoS Genetics*, *6*, e1001186.

Chen, J., Nolte, V., & Schlotterer, C. (2015). Temperature stress mediates decanalization and dominance of gene expression in *Drosophila melanogaster*. *PLoS Genetics*, *11*, e1004883.

Choi, H. M., Beck, V. A., & Pierce, N. A. (2014). Next-generation in situ hybridization chain reaction: Higher gain, lower cost, greater durability. *ACS Nano*, *8*, 4284–4294.

Chun, S., & Fay, J. C. (2011). Evidence for hitchhiking of deleterious mutations within the human genome. *PLoS Genetics*, *7*, e1002240.

Cook, T., Pichaud, F., Sonneville, R., Papatsenko, D., & Desplan, C. (2003). Distinction between color photoreceptor cell fates is controlled by *Prospero* in *Drosophila*. *Developmental Cell*, *4*, 853–864.

Crombach, A., Wotton, K. R., Jimenez-Guri, E., & Jaeger, J. (2016). Gap gene regulatory dynamics evolve along a genotype network. *Molecular Biology and Evolution*, *33*, 1293–1307.

Dokucu, M. E., Zipursky, S. L., & Cagan, R. L. (1996). *Atonal*, *rough* and the resolution of proneural clusters in the developing *Drosophila* retina. *Development*, *122*, 4139–4147.

Escudero, L. M., & Freeman, M. (2007). Mechanism of G1 arrest in the *Drosophila* eye imaginal disc. *BMC Developmental Biology*, *7*, 13.

Estes, S., & Lynch, M. (2003). Rapid fitness recovery in mutationally degraded lines of *Caenorhabditis elegans*. *Evolution*, *57*, 1022–1030.

Estes, S., Phillips, P. C., & Denver, D. R. (2011). Fitness recovery and compensatory evolution in natural mutant lines of *C. elegans*. *Evolution*, *65*, 2335–2344.

Felix, M.-A., & Barkoulas, M. (2015). Pervasive robustness in biological systems. *Nature Reviews Genetics*, *16*, 483–496.

Felsenfeld, A. L., & Kennison, J. A. (1995). Positional signaling by *hedgehog* in *Drosophila* imaginal disc development. *Development*, *121*, 1–10.

Firth, L. C., & Baker, N. E. (2005). Extracellular signals responsible for spatially regulated proliferation in the differentiating *Drosophila* eye. *Developmental Cell*, *8*, 541–551.

Firth, L. C., Bhattacharya, A., & Baker, N. E. (2010). Cell cycle arrest by a gradient of *Dpp* signaling during *Drosophila* eye development. *BMC Developmental Biology*, *10*, 28.

Fowlkes, C. C., Eckenrode, K. B., Bragdon, M. D., Meyer, M., Wunderlich, Z., Simirenko, L., … DePace, A. H. (2011). A Conserved developmental patterning network produces quantitatively different output in multiple species of *Drosophila*. *PLoS Genetics*, *7*, e1002346.

Fu, W., & Baker, N. E. (2003). Deciphering synergistic and redundant roles of *Hedgehog*, *Decapentaplegic* and *Delta* that drive the wave of differentiation in Drosophila eye development. *Development*, *130*, 5229–5239.

Fukaya, T., Lim, B., & Levine, M. (2016). Enhancer control of transcriptional bursting. *Cell*, *166*, 358–368.

Garfield, D. A., Runcie, D. E., Babbitt, C. C., Haygood, R., Nielsen, W. J., & Wray, G. A. (2013). The impact of gene expression variation on the robustness and evolvability of a developmental gene regulatory network. *PLoS Genetics*, *11*, e1001696.

Gavish, A., Shwartz, A., Weizman, A., Schejter, E., Shilo, B.-Z., & Barkai, N. (2016). Periodic patterning of the *Drosophila* eye is stabilized by the diffusible activator *Scabrous*. *Nature Communications*, *7*, 1–10.

Génétique, C.M. -M. sélection, (1983). Interspecific competition between *Drosophila melanogaster* and *Drosophila simulans*: temperature effect on competitive ability and fitness components. *Genetics Selection Evolution*, *15*, 376–378.

Gibson, G., & Reed, L. K. (2008). Cryptic genetic variation. *Current Biology*, *18*, R989–R990.

Gibson, G. (2009). Decanalization and the origin of complex disease. *Nature Reviews Genetics*, *10*, 134–140.

Goering, L. M., Hunt, P. K., Heighington, C., Busick, C., Pennings, P., Hermisson, J., … Gibson, G. (2009). Association of *orthodenticle* with natural variation for early embryonic patterning in *Drosophila melanogaster*. *Journal of Experimental Zoology*, *312B*, 841–854.

Gompel, N., Prud'homme, B., Wittkopp, P. J., Kassner, V. A., & Carroll, S. B. (2005). Chance caught on the wing: *cis*-regulatory evolution and the origin of pigment patterns in *Drosophila*. *Nature*, *433*, 481–487.

Green, R. M., Fish, J. L., Young, N. M., Smith, F. J., Roberts, B., Dolan, K., … Hallgrímsson, B. (2017). Developmental nonlinearity drives phenotypic robustness. *Nature Communications*, *8*, 1970.

Greenwood, S., & Struhl, G. (1999). Progression of the morphogenetic furrow in the *Drosophila* eye: The roles of *hedgehog*, *Decapentaplegic* and the Raf pathway. *Development*, *126*, 5795–5808.

Heberlein, U., Wolff, T., & Rubin, G. M. (1993). The TGF[beta] homolog *dpp* and the segment polarity gene *hedgehog* are required for propagation of a morphogenetic wave in the *Drosophila* retina. *Cell*, *75*, 913–926.

Heranz, H., & Cohen, S. M. (2010). MicroRNAs and gene regulatory networks: Managing the impact of noise in biological systems. *Genes & Development*, *24*, 1339–1344.

Hermisson, J., & Wagner, G. (2004). The population genetic theory of hidden variation and genetic robustness. *Genetics*, *168*, 2271–2284.

Hilbrant, M., Almudi, I., Leite, D. J., Kuncheria, L., Posnien, N., Nunes, M., & McGregor, A. P. (2014). Sexual dimorphism and natural variation within and among species in the *Drosophila* retinal mosaic. *BMC Evolutionary Biology*, *14*, 240.

Hoekstra, H. E., & Coyne, J. A. (2007). The locus of evolution: Evo devo and the genetics of adaptation. *Evolution*, *61*, 995–1016.

Ito, Y., Harigai, A., Nakata, M., Hosoya, T., Araya, K., Oba, Y., … Niimi, T. (2013). The role of *doublesex* in the evolution of exaggerated horns in the Japanese rhinoceros beetle. *Nature Neuroscience*, *14*, 561–567.

Jarman, A. P., Grell, E. H., Ackerman, L., Jan, L. Y., & Jan, Y. N. (1994). *Atonal* is the proneural gene for *Drosophila* photoreceptors. *Nature*, *369*, 398–400.

Jeong, S., Rebeiz, M., Andolfatto, P., Werner, T., True, J., & Carroll, S. B. (2008). The evolution of gene regulation underlies a morphological difference between two *Drosophila* sister species. *Cell*, *132*, 783–793.

Johnston, R. J., & Desplan, C. (2014). Interchromosomal communication coordinates intrinsically stochastic expression between alleles. *Science*, *343*, 661–665.

Johnston, R. J., Jr, Otake, Y., Sood, P., Vogt, N., Behnia, R., Vasiliauskas, D., … Desplan, C. (2011). Interlocked feedforward loops control cell-type-specific rhodopsin expression in the *Drosophila* eye. *Cell*, *145*, 956–968.

Keren, L., van Dijk, D., Weingarten-Gabbay, S., Davidi, D., Jona, G., Weinberger, A., … Segal, E. (2015). Noise in gene expression is coupled to growth rate. *Genome Research*, *25*, 1893–1902.

Kopp, A., Duncan, I., Godt, D., & Carroll, S. B. (2000). Genetic control and evolution of sexually dimorphic characters in *Drosophila*. *Nature*, *408*, 553–559.

Kozlov, K., Kosheverova, V., Kamentseva, R., Kharchenko, M., Sokolkova, A., Kornilova, E., & Samsonova, M. (2017). Quantitative analysis of the heterogeneous population of endocytic vesicles. *Journal of Bioinformatics and Computational Biology*, *10*, 1750008.

Kumar J. P. (2013). Catching the next wave: Patterning of the *Drosophila* eye by the morphogenetic furrow, in: Molecular genetics of axial patterning, growth and disease in the *Drosophila* eye. In *Molecular genetics of axial patterning* (pp. 75–97). New York, NY: Springer New York.

Kuntz, S. G., & Eisen, M. B. (2014). Drosophila embryogenesis scales uniformly across temperature in developmentally diverse species. *PLoS Genetics*, *10*, e1004293.

Landry, C. R., Wittkopp, P. J., Taubes, C. H., Ranz, J. M., Clark, A. G., & Hartl, D. L. (2005). Compensatory *cis-trans* evolution and the dysregulation of gene expression in interspecific hybrids of *Drosophila*. *Genetics*, *171*, 1813–1822.

Li, W., Ohlmeyer, J. T., Lane, M. E., & Kalderon, D. (1995). Function of protein kinase A in *hedgehog* signal transduction and *Drosophila* imaginal disc development. *Cell*, *80*, 553–562.

Li, Y., & Baker, N. E. (2001). Proneural enhancement by *Notch* overcomes Suppressor-of-Hairless repressor function in the developing *Drosophila* eye. *Current Biology*, *11*, 330–338.

Liu, F., Morrison, A. H., & Gregor, T. (2013). Dynamic interpretation of maternal inputs by the *Drosophila* segmentation gene network. *Proceedings of the National Academy of Sciences of the United States of America*, *110*, 6724–6729.

Lott, S. E., Kreitman, M., Palsson, A., Alekseeva, E., & Ludwig, M. (2007). Canalization of segmentation and its evolution in *Drosophila*. *Proceedings of the National Academy of Sciences of the United States of America*, *104*, 10926–10931.

Lucas, T., Ferraro, T., Roelens, B., De Las Heras Chanes, J., Walczak, A. M., Coppey, M., & Dostatni, N. (2013). Live imaging of bicoid-dependent transcription in Drosophila embryos. *Current Biology*, *23*, 2135–2139.

Ma, C., & Moses, K. (1995). *Wingless* and *patched* are negative regulators of the morphogenetic furrow and can affect tissue polarity in the developing *Drosophila* compound eye. *Development*, *121*, 2279–2289.

Ma, C., Zhou, Y., Beachy, P. A., & Moses, K. (1993). The segment polarity gene *hedgehog* is required for progression of the morphogenetic furrow in the developing *Drosophila* eye. *Cell*, *75*, 927–938.

Mackay, T. F. C., Richards, S., Stone, E. A., Barbadilla, A., Ayroles, J. F., Zhu, D., Casillas, S., … Gibbs, R. A. (2012). The *Drosophila* melanogaster genetic reference panel. *Nature*, *482*, 173–178.

MacNeil, L. T., & Walhout, A. J. M. (2011). Gene regulatory networks and the role of robustness and stochasticity in the control of gene expression. *Genome Research*, *21*, 645–657.

Maisnier-Patin, S., & Andersson, D. I. (2004). Adaptation to the deleterious effects of antimicrobial drug resistance mutations by compensatory evolution. *Research in Microbiology*, *155*, 360–369.

Marinov, G. K., Williams, B. A., McCue, K., Schroth, G. A., Gertz, J., Myers, R. M., & Wold, B. J. (2014). From single-cell to cell-pool transcriptomes: Stochasticity in gene expression and RNA splicing. *Genome Research*, *24*, 496–510.

McKenzie, J. A. (1993). Measuring fitness and intergenic interactions: The evolution of resistance to diazinon in *Lucilia cuprina*. *Genetica*, *90*, 227–237.

McKenzie, J. A., & Clarke, G. M. (1988). Diazinon resistance, fluctuating asymmetry and fitness in the Australian sheep blowfly, *Lucilia cuprina*. *Genetics*, *120*, 213–220.

McKenzie, J. A., Whitten, M. J., & Adena, M. A. (1982). The effect of genetic background on the fitness of diazinon resistance genotypes of the Australian sheep blowfly, *Lucilia cuprina*. *Heredity*, *49*, 1–9.

Meyer, F. (1994). Topographic distance and watershed lines. *Signal processing*, *38*, 113–125.

Moore, F. B., Rozen, D. E., & Lenski, R. E. (2000). Pervasive compensatory adaptation in *Escherichia coli*. *Proceedings of the Royal Society B*, *267*, 515–522.

Namba, R., Pazdera, T. M., Cerrone, R. L., & Minden, J. S. (1997). *Drosophila* embryonic pattern repair: How embryos respond to *bicoid* dosage alteration. *Development*, *124*, 1393–1403.

Nijhout, H. F., Sadre-Marandi, F., Best, J., & Reed, M. C. (2017). Systems biology of phenotypic plasticity and robustness. *Integrative and Comparative Biology*, *57*, 171–184.

Paaby, A., & Gibson, G. (2016). Cryptic genetic variation in evolutionary developmental genetics. *Biology*, *5*, 28–13.

Paaby, A. B., & Rockman, M. V. (2014). Cryptic genetic variation: Evolution's hidden substrate. *Nature Reviews Genetics*, *15*, 247–258.

Pai, A. A., & Gilad, Y. (2014). Comparative studies of gene regulatory mechanisms. *Current Opinion in Genetics & Development*, *29*, 68–74.

Pai, A. A., Pritchard, J. K., & Gilad, Y. (2015). The genetic and mechanistic basis for variation in gene regulation. *PLoS Genetics*, e1004857.

Pan, D., & Rubin, G. M. (1995). CAMP-dependent protein kinase and *hedgehog* act antagonistically in regulating decapentaplegic transcription in *Drosophila* imaginal discs. *Cell*, *80*, 543–552.

Parks, A. L., Turner, F. R., & Muskavitch, M. A. (1995). Relationships between complex *Delta* expression and the specification of retinal cell fates during *Drosophila* eye development. *Mechanisms of Development*, *50*, 201–216.

Raj, A., van den Bogaard, P., Rifkin, S. A., van Oudenaarden, A., & Tyagi, S. (2008). Imaging individual mRNA molecules using multiple singly labeled probes. *Nature Methods*, *5*, 877–879.

Raj, A., & van Oudenaarden, A. (2008). Stochastic gene expression and its consequences. *Cell*, *135*, 216–226.

Reed, R. D., Papa, R., Martin, A., Hines, H. M., Counterman, B. A., Pardo-Diaz, C., … McMillan, W. O. (2011). *optix* drives the repeated convergent evolution of butterfly wing pattern mimicry. *Science*, *333*, 1137–1141.

Roignant, J.-Y., & Treisman, J. E. (2009). Pattern formation in the *Drosophila* eye disc. *The International Journal of Developmental Biology*, *53*, 795–804.

Romero, I. G., Ruvinsky, I., & Gilad, Y. (2012). Comparative studies of gene expression and the evolution of gene regulation. *Nature Reviews Genetics*, *13*, 505–516.

Rosenblum, E. B., Römpler, H., Schöneberg, T., & Hoekstra, H. E. (2010). Molecular and functional basis of phenotypic convergence in white lizards at White Sands. *Proceedings of the National Academy of Sciences of the United States of America*, *107*, 2113–2117.

Rutherford, S., Yoshikazu, H., & Swalla, B. J. (2007). The Hsp90 capacitor, developmental remodeling, and evolution: The robustness of gene networks and the curious evolvability of metamorphosis. *Critical Reviews in Biochemistry and Molecular Biology*, *42*, 355–372.

Shah, S., Lubeck, E., Schwarzkopf, M., & He, T. F. (2016). Single-molecule RNA detection at depth via hybridization chain reaction and tissue hydrogel embedding and clearing. *Development*, *143*, 2862–2867.

Signor, S. A., Liu, Y., Rebeiz, M., & Kopp, A. (2016). Genetic convergence in the evolution of male-specific color patterns in *Drosophila*. *Current Biology*, *26*, 2423–2433.

Signor, S. A., New, F. N., & Nuzhdin, S. (2017). A Large panel of *Drosophila simulans* reveals an abundance of common variants. *Genome Biology and Evolution*, *10*, 189–206.

Signor, S. A., & Nuzhdin, S. (2018). Dynamic changes in gene expression and alternative splicing mediate the response to acute alcohol exposure in *Drosophila melanogaster*. *Heredity*, *121*, 342–360.

Spencer, S. A., Powell, P. A., Miller, D. T., & Cagan, R. L. (1998). Regulation of EGF receptor signaling establishes pattern across the developing *Drosophila* retina. *Development*, *125*, 4777–4790.

Stern, D. L. (2000). Evolutionary developmental biology and the problem of variation. *Evolution*, *54*, 1079–1091.

Stoebel, D. M., Hokamp, K., Last, M. S., & Dorman, C. J. (2009). Compensatory evolution of gene regulation in response to stress by *Escherichia coli* lacking RpoS. *PLoS Genetics*, *5*, e1000671.

Strutt, D. I., & Mlodzik, M. (1997). *Hedgehog* is an indirect regulator of morphogenetic furrow progression in the *Drosophila* eye disc. *Development*, *124*, 3233–3240.

Sun, Y., Jan, L. Y., & Jan, Y. N. (1998). Transcriptional regulation of *atonal* during development of the *Drosophila* peripheral nervous system. *Development*, *125*, 3731–3740.

Szamecz, B., Boross, G., Kalapis, D., Kovács, K., Fekete, G., Farkas, Z., … Pál, C. (2014). The genomic landscape of compensatory evolution. *PLoS Biology*, *12*, e1001935.

Tantale, K., Kozulic-Pirher, A., Lesne, A., Victor, J. M., Robert, M. C., Capozi, S., … Bertrand, E. (2016). A single-molecule view of transcription reveals convoys of RNA polymerases and multi-scale bursting. *Nature Communications*, *7*, 1–14.

Thompson, A., Zakon, H. H., & Kirkpatrick, M. (2015). Compensatory drift and the evolutionary dynamics of dosage-sensitive duplicate genes. *Genetics*, *202*, 765–774.

True, J. R., & Haag, E. S. (2001). Developmental system drift and flexibility in evolutionary trajectories. *Evolution & Development*, *3*, 1–11.

Tsachaki, M., & Sprecher, S. G. (2011). Genetic and developmental mechanisms underlying the formation of the *Drosophila* compound eye. *Developmental Dynamics*, *241*, 40–56.

Vincent, L. (1993). Morphological grayscale reconstruction in image analysis: Applications and efficient algorithms. *IEEE Transactions on Image Processing*, *2*, 176–201.

Wernet, M. F., Mazzoni, E. O., Çelik, A., Duncan, D. M., Duncan, I., & Desplan, C. (2006). Stochastic spineless expression creates the retinal mosaic for colour vision. *Nature*, *440*, 174–180.

Wotton, K. R., Jimenez-Guri, E., Crombach, A., Janssens, H., Alcaine-Colet, A., Lemke, D., … Jaeger, J. (2015). Quantitative system drift compensates for altered maternal inputs to the gap gene network of the scuttle fly *Megaselia abdita*. *Elife*, *4*, 1–28.

Wray, G. A. (2007). The evolutionary significance of cis-regulatory mutations. *Nature Reviews Genetics*, *8*, 206–216.

Wunderlich, Z., Bragdon, M. D., Eckenrode, K. B., Lydiard-Martin, T., Pearl-Waserman, S., & DePace, A. H. (2012). Dissecting sources of quantitative gene expression pattern divergence between *Drosophila* species. *Molecular Systems Biology*, *8*, 1–15.

Yassin, A., Delaney, E. K., Reddieux, A., Bastide, H., Seher, T., Appleton, N. C., … Kopp, A. (2016). *pdm3* is responsible for recurrent evolution of female-limited color dimorphism in *Drosophil*. *Current Biology*, *26*, 2412–2422.

SUPPORTING INFORMATION

Additional supporting information may be found online in the Supporting Information section at the end of the article.

How to cite this article: Ali S, Signor SA, Kozlov K, Nuzhdin SV. Novel approach to quantitative spatial gene expression uncovers genetic stochasticity in the developing *Drosophila* eye. *Evolution & Development*. 2019;1–15. https://doi.org/10.1111/ede.12283